IDENTIFICATION OF A RANDOM ELASTIC MEDIUM BY VIBRATION TESTS

C. Desceliers
University of Marne-la-vallée, Paris, France
christophe.desceliers@univ-mlv.fr

C. Soize
University of Marne-la-vallée, Paris, France
soize@univ-mlv.fr

Abstract. *This paper deals with the experimental identification of the probabilistic representation of a random field modeling the Young modulus of a non homogeneous isotropic elastic medium by experimental vibration tests. The experimental database is constiturted of the frequency response functions measured on a part of the boundary of a given set of specimen. Realisations of the random field modelling the Young modulus are then identified setting an inverse problem for each specimen. The random field representation modelling the Young modulus is consgtructed and is based on the polynomial chaos decomposition. The coefficients of the polynomial chaos decomposition are identified in solving an optimization problem related to the maximum likelihood principle. For the presented example, this method allows the probability density functions and the autocorrelation functions to be identified.*

Keywords:*Random elastic medium, identification, polynomial chaos*

1. Introduction

For elastic random media (see for instance Spanos and Ghanem (1989)), a fundamental question concerns the experimental identification of the probabilistic model of the elastic properties. Generally, identification of random parameters involves a stochastic inverse problem to be solved (see for instance Fadale and al (1995), Shevtsov (1999) and Cappilla *et al* (2000)). In a recent work proposed by Desceliers, Ghanem and Soize (2004), this problem addressed : (1) A polynomial chaos representation of random fields to be identified is used. (2) An estimation of the coefficients of the chaos representation is performed by using the maximum likelihood method. (3) The experimental test is assumed to be static which generaly requires a lot of experimental measurements for a very heterogeneous random medium. In this paper, we present an extension of this method in the context of experimental vibrational tests. The objective is (1) to use the mesurements of the response in a frequency band which allows the quality of the construction to be incereased with respect to static measurements and (2) to have a method based on the use of vibrational tests instead of static tests.

2. Presentation of the method

The proposed method is presented through a simple example related to the experimental identification of the random field modeling the Young modulus ofa random linear isotropic heterogeneous medium by vibrational tests. The data used for the identification correspond to experimental measurements of the frequency response functions related to the displacement field on the boundary of the specimen. In a first step, the proposed method consists in estimating the Young modulus field of each specimen. For this, the elastodynamic problem is written for the specimen and is discretized by the finite element method. The random Young modulus field is then projected on the finite element basis for which the random coefficients have to be identified. For each specimen the realization of the random coefficients are calculated by solving a first optimization problem allowing the norm between the measured and the calculated response functions of the specimen to be minimized. In a second step, these random coefficients whose realizations have been constructed, are then represented by using the polynomial chaos representation (see for instance Wiener, 1938, Ghanem and Spanos, 1991, Soize and Ghanem, 2003). In a last step, a second optimization problem allows the coefficients to be calculated by using the maximum likelihood method. Consequently, the probabilistic model of the random Young modulus field is completely defined.

3. Construction of an "experimental data basis" by Monte Carlo numerical simulation of the direct problem

In this paper, the «experimental databas» is constructed by numerical simulation. The specimen is constituted of a non-homogeneous isotropic linear elastic medium occupaying a three-dimensional bounded domain $\mathcal{D}$ with boundary $\partial\mathcal{D}$ given in a Cartesian system $Ox_1x_2x_3$. The geometry of domain $\mathcal{D}$ is a slender rectangular box shown in Figure 1 whose dimensions along x_1, x_2 and x_3 are $L_1 = 1.3 \times 10^{-1} m$, $L_2 = 2 \times 10^{-2} m$ and $L_3 = 2 \times 10^{-2} m$. The structure is fixed on the part Γ_0 of $\partial\mathcal{D}$ for which the displacement field is zero.

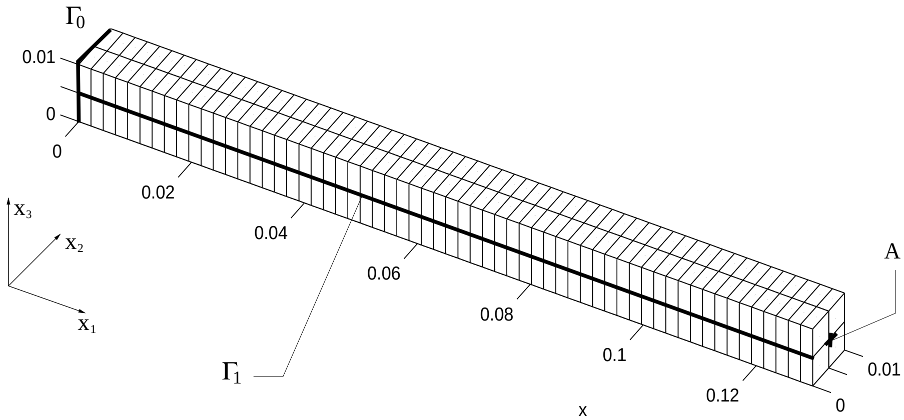

Figure 1. Definition of the specimen

The structure is subjected to an external point force denoted as $\mathbf{b}(t)$ and applied to the node A along $x_1 - axis$ (see Fig. 1). The Fourier transform $\widehat{\mathbf{b}}$ of $\mathbf{b}$ is the constant vector $(1, 0, 0)$ in the frequency band $[0, 50]$ kHz. The viscoelastic medium is random. It is assumed that only the random parameter is the Young modulus. In reality, we should consider the Poisson coefficient also as random parameter. This assumption is introduced in order to simplify the presentation. The random Young modulus field is modeled by a positive-valued second-order random field $Y(\mathbf{x})$ defined by

$$Y(\mathbf{x}) = c_0\, g(c_1, c_2\, V(\mathbf{x})) \quad , \quad \forall \mathbf{x} \in \mathcal{D} \tag{1}$$

in which $c_0 = 1.6663 \times 10^{10}\ N.m^{-2}$, $c_1 = 1.5625$ and $c_2 = 0.2$. The function $u \mapsto g(\alpha, u)$ from $\mathbb{R}$ into $]0\,, +\infty[$ is such that, for all u in $\mathbb{R}$,

$$h(\alpha, u) = F_{\Gamma_\alpha}^{-1}(F_U(u)) \quad ,$$

in which $u \mapsto F_U(u) = P(U \leq u)$ is the cumulative distribution function of the normalized Gaussian random variable U and where the function $p \mapsto F_{\Gamma_\alpha}^{-1}(p)$ from $]0\,, 1[$ into $]0\,, +\infty[$ is the reciprocal function of the cumulative distribution function $\gamma \mapsto F_{\Gamma_\alpha}(\gamma) = P(\Gamma_\alpha \leq \gamma))$ of the gamma random variable Γ_α with parameter α. In the right-hand side of Eq. (1) , $\{V(\mathbf{x}), \mathbf{x} \in \mathcal{D}\}$ is a second-order random field such that $E\{V(\mathbf{x})\} = 0$ and $E\{V(\mathbf{x})^2\} = 1$, defined by

$$V(\mathbf{x}) = \sum_{|\boldsymbol{\alpha}|=1}^{3} H_{\boldsymbol{\alpha}}(z_1, z_2, z_3, z_4)\, \sqrt{\gamma_{\boldsymbol{\alpha}}}\, \psi_{\boldsymbol{\alpha}}(\mathbf{x}/2) \quad , \tag{2}$$

in which $\{z_1, z_2, z_3, z_4\}$ are independent normalized Gaussian random variables, $\boldsymbol{\alpha}$ is a multi-index $(\alpha_1, \alpha_2, \alpha_3, \alpha_4) \in \mathbb{N}^4$, $|\boldsymbol{\alpha}| = \alpha_1 + \alpha_2 + \alpha_3 + \alpha_4$ and where $H_{\boldsymbol{\alpha}}(z_1, z_2, z_3, z_4) = H_{\alpha_1}(z_1) \times H_{\alpha_2}(z_2) \times H_{\alpha_3}(z_3) \times H_{\alpha_4}(z_4)$ in which $H_{\alpha_k}(z_k)$ is the normalized Hermite polynomial of order α_k such that

$$\int_{\mathbb{R}} H_{\alpha_k}(w)\, H_{\alpha_j}(w) \frac{1}{\sqrt{2\pi}} e^{-\frac{1}{2}w^2}\, dw = \delta_{\alpha_k \alpha_j} \ .$$

In the right-hand side of Eq. (2) , $\{\gamma_{\boldsymbol{\alpha}}\}_{1 \leq |\boldsymbol{\alpha}| \leq 3}$ and $\{\psi_{\boldsymbol{\alpha}}\}_{1 \leq |\boldsymbol{\alpha}| \leq 3}$ are defined as the eigenvalues and the eigeinfunctions of the the integral linear operator **C** defined by the kernel $C(\mathbf{x}, \mathbf{x}') = \exp(-|x_1 - x_1'|/L)$ in which $L = L_1/40$ and where $\mathbf{x} = (x_1, x_2, x_3)$ and $\mathbf{x}' = (x_1', x_2', x_3')$ belong to $\mathcal{D}$. This means that the **correlation length** of the random field is much smaller than the length L_1 of the specimen. The eigenvalue problem related to operator **C** is then written as

$$\int_{\mathcal{D}} C(\mathbf{x}, \mathbf{x}') \psi_{\boldsymbol{\alpha}}(\mathbf{x}') d\mathbf{x}' = \gamma_{\boldsymbol{\alpha}} \psi_{\boldsymbol{\alpha}}(\mathbf{x}) \quad . \tag{3}$$

It should be nofted that, $Y(\mathbf{x}) = Y(x_1)$ and consequently, $Y(\mathbf{x})$ is independent of x_2 and x_3. Figure 2 shows the mean value $\mathbf{x} \mapsto E\{Y(\mathbf{x})\}$ where $E\{\}$ denotes the mathematical expectation. Figure 3 shows the graph of the normalized cautocorrelation function $(\mathbf{x}, \mathbf{x}') \mapsto E\{Y(\mathbf{x})Y(\mathbf{x}')\}/(E\{Y(\mathbf{x})\}\, E\{Y(\mathbf{x}')\})$. Finally, it is assumed that the Poisson coefficient $\mu = 0.3$ and the mass density $\rho = 2.7 \times 10^3\ Kg/m^3$ are deterministic real constants.

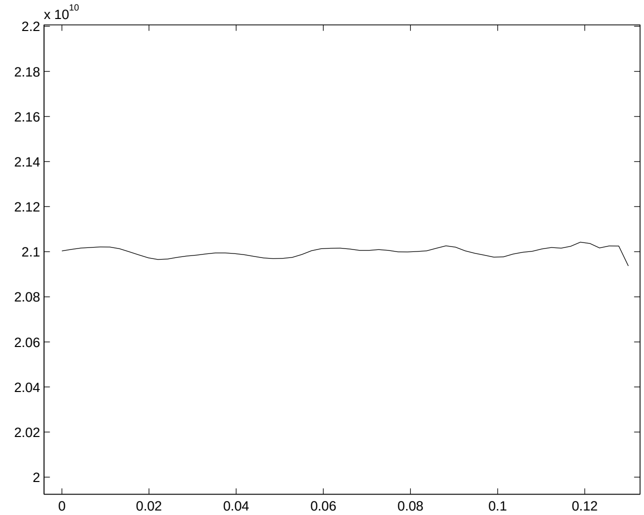

Figure 2. Graph of the function $\mathbf{x} \mapsto E\{Y(\mathbf{x})\}$ where $\mathbf{x} = (x_1, x_2, x_3)$ with $x_2 = x_3 = 0$. Horizontal axis: x_1. Vertical axis: $E\{Y(\mathbf{x})\}$.

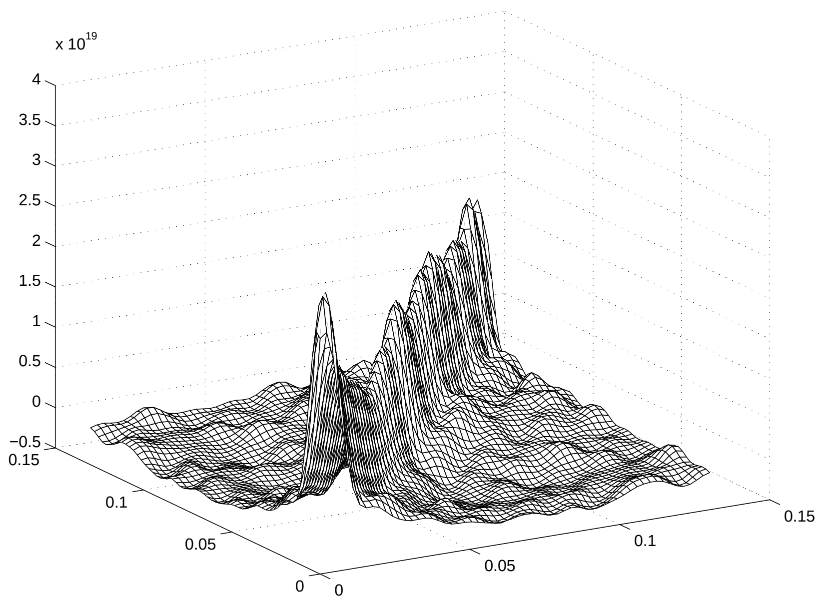

Figure 3. Graph of the function $(\mathbf{x}, \mathbf{x}') \mapsto E\{Y(\mathbf{x})Y(\mathbf{x}')\}/(E\{Y(\mathbf{x})\}\, E\{Y(\mathbf{x}')\})$ where $\mathbf{x} = (x_1, x_2, x_3)$ and $\mathbf{x}' = (x'_1, x'_2, x'_3)$ with $x_2 = x_3 = 0$ and $x'_2 = x'_3 = 0$. Horizontal axis: x_1 and x'_1. Vertical axis: $E\{Y(\mathbf{x})Y(\mathbf{x}')\}/(E\{Y(\mathbf{x})\}\, E\{Y(\mathbf{x}')\})$.

The finite element mesh of the structure is shown in Fig. 1 and consists of 8-node isoparametric 3D solid finite elements. There are $N_d = 1620$ degrees of freedom. Let $\mathbf{z} = (z_1, z_2, z_3, z_4)$ be the $\mathbb{R}^4$-valued random variable constituted of the 4 independent random variables appearing in Eq. (2) (the random germ of uncertainties). Let $[K(\mathbf{z})]$ be the random stiffness matrix with values in the set of all the positive-definite symmetric $(N_d \times N_d)$ real matrices. Let $[M]$ and $[D]$ be the mass and the damping matrices such that $[D] = a\,[M]$ with $a = 10^3\,Hz$. Matrices $[M]$ and $[D]$ are the deterministic positive-definite symmetric $(N_d \times N_d)$ real matrices. The $\mathbb{R}^{N_d}$-valued random vector of the frequency response function related to the nodal displacements is denoted by $\mathbf{X}(\omega)$ and is such that

$$[A(\omega;\mathbf{z})]\mathbf{X}(\omega) = \mathbf{f}(\omega) \quad ,$$

in which $[A(\omega;\mathbf{z})]$ is the dynamic stiffness matrix such that $[A(\omega;Y)] = -\omega^2\,[M] + i\,\omega\,[D] + [K(\mathbf{z})]$ and where $\mathbf{f}(\omega)$ is the $\mathbb{R}^{\mathbb{N}_d}$-vectore of the external forces. Let $\mathbf{X}_\Gamma(\omega)$ be the vector corresponding to the $N_b = 60$ nodes belonging to $\partial\mathcal{D}$ which can be written as $\mathbf{X}_\Gamma(\omega) = \mathbb{P}(\mathbf{X}(\omega))$ in which $\mathbb{P}$ is a linear mapping from $\mathbb{R}^{\mathbb{N}_d}$ into $\mathbb{R}^{\mathbb{N}_b}$. The experimental database is constituted of $m = 100$ realizations of random vector $\mathbf{X}_\Gamma(\omega)$ denoted by $\mathbf{X}_\Gamma^1 = \mathbf{X}_\Gamma(\theta_1), \ldots, \mathbf{X}_\Gamma^m = \mathbf{X}_\Gamma(\theta_m)$, and corresponding to the specimen.

4. Identification of the random field modeling the Young modulus by solving an inverse problem

The finite element approximation $\widetilde{Y}$ of random field Y indexed by $\mathcal{D}$ is written as $\widetilde{Y}(\mathbf{x}) = \sum_{k=1}^{N} R_k h_k(x_1)$ in which $h_1(x_1), \ldots, h_N(x_1)$ are the usual linear interpolation functions related to the finite element mesh of domain $\mathcal{D}$, where $N = 60$ is the degree of this approximation and where $R_1, \ldots R_N$ are the random coefficients. We introduce the $\mathbb{R}^N$-valued random variable $\mathbf{R}$ such that $\mathbf{R} = (R_1, \ldots, R_N)$. Let $[\widetilde{A}(\omega; \mathbf{R})]$ be the random dynamical stiffness matrix constructed by using the finite element approximations $\widetilde{Y}(\mathbf{x})$ of the Young modulus. For each realization $\mathbf{X}_\Gamma^j$ belonging to the experimental database, the realization $\mathbf{R}^j = \mathbf{R}(\theta_j)$ of the random variable $\mathbf{R}$ are constructed by solving the nonlinear optimization problem

$$\min_{\mathbf{R}^j} \ell_{dyn}(\mathbf{R}^j, \mathbf{X}_\Gamma^j) \quad , \tag{4}$$

in which

$$\ell_{dyn}(\mathbf{R}^j, \mathbf{X}_\Gamma^j) = \sum_{k=1}^{N_{band}} \int_{B_k} \left\| \mathbb{P}\left([\widetilde{A}(\omega; \mathbf{R})]^{-1} \mathbf{f}(\omega) \right) - \mathbf{X}_\Gamma^j(\omega) \right\|^2 d\omega \quad .$$

In the right-hand side of Eq. (4) , $B_k = [\omega_{\min,k}, \omega_{\max,k}]$ with $\omega_{\min,k} = \omega_k - B_{eq,k}/2$ and $\omega_{\min,k} = \omega_k + B_{eq,k}/2$ where $B_{eq,k} = a\,\pi \sqrt{1 - (a/(2\omega_k)^2)}$ in the equivalent bandwidth related to the eigenfrequency ω_k of the mean model of the specimens and where N_band is the number of bands considered for the identification. It should be noted that the problem of optimization introduced by Desceliers and Ghanem and Soize, 2004 in order to solve the inverse problem to calculate the realisations $\mathbf{R}^1, \ldots, \mathbf{R}^m$ of random vector $\mathbf{R}$ is based on an elastostatic problem. In this case, the experimental database is constituted of static measurements and the optimisation problem is

$$\min_{\mathbf{R}^j} \ell_{stat}(\mathbf{R}^j, \mathbf{X}_\Gamma^j) \quad , \tag{5}$$

in which

$$\ell_{stat}(\mathbf{R}^j, \mathbf{X}_\Gamma^j) = \left\| \mathbb{P}\left([\widetilde{A}(0; \mathbf{R})]^{-1} \mathbf{f}(0) \right) - \mathbf{X}_\Gamma^j(0) \right\|^2 \quad .$$

The optimization problems defined by Eqs (4) and (5) are solved least-squares estimation of nonlinear parameters (see, Marquardt, 1963). Finally, for all $\mathbf{x}$ fixed in $\mathcal{D}$, the realizations $\widetilde{Y}^1(\mathbf{x}) = \widetilde{Y}(\mathbf{x}; \theta_1), \ldots, \widetilde{Y}^m(\mathbf{x}) = \widetilde{Y}(\mathbf{x}; \theta_m)$ of random variable $\widetilde{Y}(\mathbf{x})$ are constructed by using the relation $\widetilde{Y}^j(\mathbf{x}) = \mathbf{h}(x_1)^T \mathbf{R}^j$ in which $\mathbf{h}(x_1) = (h_1(x_1), \ldots, h_N(x_1))$. Figure 4 shows the graph of realization $x_1 \mapsto \widetilde{Y}^1(\mathbf{x})$ with $x_2 = x_3 = 0$ constructed by solving Eqs (4) («dynamic inverse problem») and (5) («static inverse problem»). It can be seen that the dynamical inverse problem gives results more accurated than the statistical inverse problem. This can be explained by considering the dynamical inverse problem as the set of a great number of static inverse problem with different loading case $F(\omega)$, frequency ω belonging to $\cup_{k=1}^{N_{band}} B_k$.

5. Statistical reduction

The size of the random vector $\mathbf{R}$ can be reduced. Let $\lambda_1 \geq \ldots \geq \lambda_N$ be the eigenvalues of the covariance matrix $[C_\mathbf{R}]$ of random vector $\mathbf{R}$. The normalized eigenvectors associated with the eigenvalues $\lambda_1, \ldots, \lambda_N$ are denoted by $\boldsymbol{\varphi}_1, \ldots, \boldsymbol{\varphi}_N$. Consequently, the random vector $\mathbf{R}$ can be written as

$$\mathbf{R} = \underline{\mathbf{R}} + \sum_{k=1}^{N} Q_k \sqrt{\lambda_k} \boldsymbol{\varphi}_k \quad ,$$

in which $Q_1, \ldots, Q_N$ are N centered real-valued random variables defined by $\sqrt{\lambda_k} Q_k = \langle \mathbf{R} - \underline{\mathbf{R}}, \boldsymbol{\varphi}_k \rangle_{\mathbb{R}^N}$ where $\underline{\mathbf{R}} = E\{\mathbf{R}\}$ such that for all k and ℓ, $E\{Q_k\} = 0$ and $E\{Q_k Q_\ell\} = \delta_{k\ell}$. Figure 5 displays the graph of the function $n \mapsto \sum_{k=1}^{n} \lambda_k^2$. It can be deduced that random vector $\mathbf{R}$ can be approximated by the random vector $\underline{\mathbf{R}} + [\Phi]\,[\Lambda]\mathbf{Q}^\mu$ with $\mu = 15 < N$ in which the $(\mu \times \mu)$ matrix $[\Lambda]$ and the $(N \times \mu)$ matrix $[\Phi]$ are such that $[\Lambda]_{\ell k} = \delta_{\ell k} \sqrt{\lambda_\ell}$ and $[\Phi]_{\ell k} = \varphi_{k,\ell}$ in which $\boldsymbol{\varphi}_k = (\varphi_{k,1}, \ldots, \varphi_{k,N})$ and where $\mathbf{Q}^\mu = (Q_1, \ldots, Q_\mu)$. For all $j = 1, \ldots, m$, the realization $\mathbf{q}^j = \mathbf{Q}^\mu(\theta_j)$ of random vector $\mathbf{Q}^\mu$ is calculated by $\mathbf{q}^j = [\Lambda]^{-1}[\Phi]^T(\mathbf{R}^j - \underline{\mathbf{R}})$.

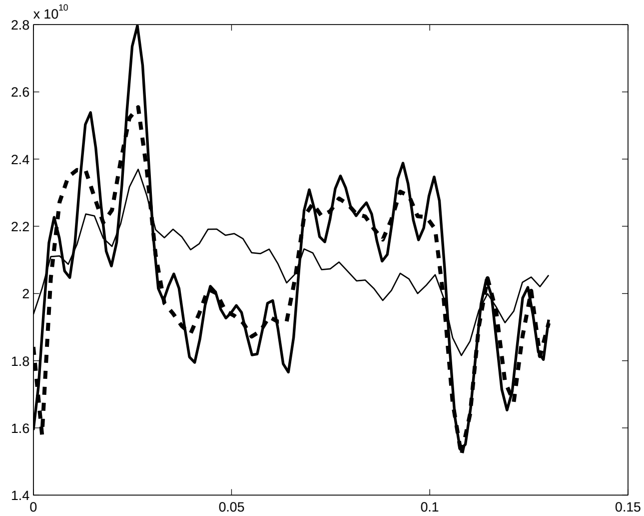

Figure 4. Graph of $x_1 \mapsto Y(\mathbf{x};\theta_1)$ (thick solid line) and graph of realization $x_1 \mapsto \widetilde{Y}^1(\mathbf{x})$ with $x_2 = x_3 = 0$ constructed by solving the «dynamic inverse problem» (dash lines) with $N_{band} = 5$ and the «static inverse problem» (thin solid lines). Horizontal axis: x_1. Vertical axis: $Y(\mathbf{x};\theta_1)$ and $\widetilde{Y}^1(\mathbf{x})$

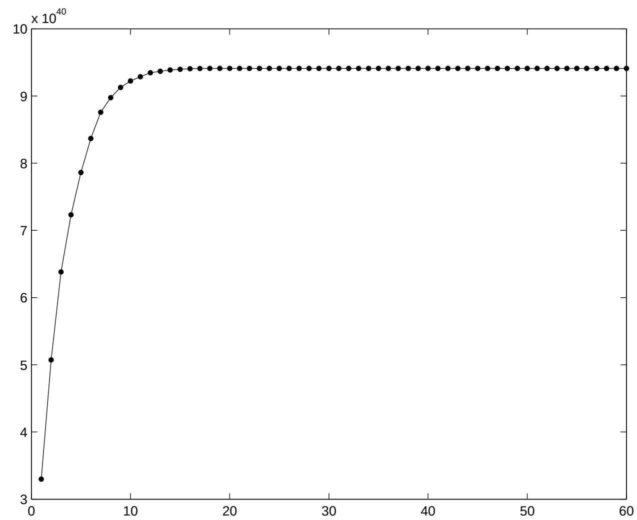

Figure 5. Convergence analysis of the statistical reduction : graph of function $n \mapsto \sum_{k=1}^{n} \lambda_k^2$. Horizontal axis n, vertical axis $\sum_{k=1}^{n} \lambda_k^2$.

6. Chaos decomposition

Let $\mathbf{W}^\nu = (W_1, \ldots, W_\nu)$ be the normalized Gaussian random vector such that $E\{W_i W_j\} = \delta_{ij}$. The truncated Chaos representation of the $\mathbb{R}^\mu$-valued random variable $\mathbf{Q}^\mu$ in terms of $\mathbf{W}^\nu$ is written as

$$\mathbf{Q}^{\mu,\nu} = \sum_{\boldsymbol{\alpha},|\boldsymbol{\alpha}|=1}^{+\infty} \mathbf{a}_{\boldsymbol{\alpha}} H_{\boldsymbol{\alpha}}(\mathbf{W}^\nu) \quad , \tag{6}$$

where $\boldsymbol{\alpha}$ is a multi-index belonging to $\mathbb{N}^\nu$ and where $H_{\boldsymbol{\alpha}}(\mathbf{W}^\nu)$ is the multi-indexed Hermite polynomials (see section 3). The coefficients $\mathbf{a}_{\boldsymbol{\alpha}}$ belonging to $\mathbb{R}^\mu$ are such that $\sum_{\boldsymbol{\alpha},|\boldsymbol{\alpha}|=1}^{+\infty} \mathbf{a}_{\boldsymbol{\alpha}} \mathbf{a}_{\boldsymbol{\alpha}}^T = [I_\mu]$ in which $[I_\mu]$ is the $(\mu \times \mu)$ unit matrix. The truncated Chaos representation of random vector $\mathbf{Q}^{\mu,\nu}$ is denoted by $\mathbf{Q}^{\mu,\nu,d}$ and is such that $\mathbf{Q}^{\mu,\nu,d} = \sum_{\boldsymbol{\alpha},|\boldsymbol{\alpha}|=1}^{d} \mathbf{a}_{\boldsymbol{\alpha}} H_{\boldsymbol{\alpha}}(\mathbf{W}^\nu)$. Finally, for all $\mathbf{x} \in \mathcal{D}$, random Young modulus $\widetilde{Y}(\mathbf{x})$ can be approximated by the random variable $\widetilde{Y}^{\mu,\nu,d}(\mathbf{x}) = \mathbf{h}(x_1)^T\,[\Phi]\,[\Lambda]\mathbf{Q}^{\mu,\nu,d} + \mathbf{h}(x_1)^T\,\underline{\mathbf{R}}$.

The maximum likelihood method (see for instance Serfling, 1980) is used in order to estimate, from realisations $\mathbf{q}^1, \ldots, \mathbf{q}^m$, parameters $\boldsymbol{a}_{\boldsymbol{\alpha}}$. We then have to solve the following problem of optizimation: find $\mathbb{A} = \{\mathbf{a}_{\boldsymbol{\alpha}}, |\boldsymbol{\alpha}| = 1, \ldots, d\}$

such that

$$\max_{\mathbb{A}} L(\mathbf{q}^1,\ldots,\mathbf{q}^m;\mathbb{A}) \quad , \quad \text{such that} \quad \sum_{\boldsymbol{\alpha},|\boldsymbol{\alpha}|=1}^{d} \mathbf{a}_{\boldsymbol{\alpha}}\mathbf{a}_{\boldsymbol{\alpha}}^T = [\,I_\mu] \tag{7}$$

where $L(\mathbf{q}^1,\ldots,\mathbf{q}^m;\mathbb{A}) = p_{\mathbf{Q}^{\mu,\nu,d}}(\mathbf{q}^1,\mathbb{A})\times\ldots\times p_{\mathbf{Q}^{\mu,\nu,d}}(\mathbf{q}^m,\mathbb{A})$ denotes the likelihood function associated with observations $\mathbf{q}^1,\ldots,\mathbf{q}^m$ and where $p_{\mathbf{Q}^{\mu,\nu,d}}$ is the probability density function of $\mathbf{Q}^{\mu,\nu,d}$. However, the optimization problem defined by Eq. (7) yields a very high computational cost induced by the estimation of the joint probability density functions $p_{\mathbf{Q}}^{\mu,\nu,d}(\mathbf{q}^j,\mathbf{a})$, for reasonable values of the length μ of random vector $\mathbf{Q}^{\mu,\nu,d}$. Consequently, it is proposed to substitute the usual likelihood function by the pseudo-likelihood function

$$\widetilde{L}(\mathbf{q}^1,\ldots,\mathbf{q}^m;\mathbb{A}) = \prod_{k=1}^{\mu} p_{Q_k^{\mu,\nu,d}}(q_k^1,\mathbb{A})\times\ldots\times\prod_{k=1}^{\mu} p_{Q_k^{\mu,\nu,d}}(q_k^m,\mathbb{A}) \tag{8}$$

where $\mathbf{q}^j = (q_1^j,\ldots,q_\mu^j)$ and $\mathbf{Q}^{\mu,\nu,d} = (Q_1^{\mu,\nu,d},\ldots,Q_\mu^{\mu,\nu,d})$ and where $p_{Q_k^{\mu,\nu,d}}$ is the probability density function of $Q_k^{\mu,\nu,d}$. Finally, the following problem of optimization is substituted to the problem defined by Eq. (7) . Find $\mathbb{A} = \{\mathbf{a}_{\boldsymbol{\alpha}}, |\boldsymbol{\alpha}| = 1,\ldots,d\}$ such that

$$\max_{\mathbb{A}} \widetilde{L}(\mathbf{q}^1,\ldots,\mathbf{q}^m;\mathbb{A}) \quad , \quad \text{such that} \quad \sum_{\boldsymbol{\alpha},|\boldsymbol{\alpha}|=1}^{d} \mathbf{a}_{\boldsymbol{\alpha}}\mathbf{a}_{\boldsymbol{\alpha}}^T = [\,I_\mu] \quad . \tag{9}$$

7. Convergence Analysis

In order to perform a convergence analysis of the method proposed in this paper, the normalized stochastic fields $\varepsilon(\mathbf{x})$ and $\tilde{\varepsilon}^{\mu,\nu,d}$ defined by, for all $\mathbf{x}\in\mathcal{D}$, $\varepsilon(\mathbf{x}) = Y(\mathbf{x})/E\{Y(\mathbf{x})\}$ and $\tilde{\varepsilon}^{\mu,\nu,d}(\mathbf{x}) = Y^{\mu,\nu,d}(\mathbf{x})/E\{Y^{\mu,\nu,d}(\mathbf{x})\}$ are introduced. Figure 6 shows the graphs of functions $\mathbf{x}\mapsto E\{\varepsilon(\mathbf{x})\varepsilon(\mathbf{x}')\}$ (thick dashed lines) and $\mathbf{x}\mapsto E\{\varepsilon^{\mu,\nu,d}(\mathbf{x})\varepsilon^{\mu,\nu,d}(\mathbf{x}')\}$ where $\mathbf{x} = (x_1,x_2,x_3)$ and $\mathbf{x}' = (x_1',x_2',x_3')$ with $x_2 = x_3 = 0$ and $x_2' = x_3' = 0$, for $x_1' = 0.0173$ (Fig. 6a), $x_1' = 0.0520$ (Fig. 6b), $x_1' = 0.0888$ (Fig. 6c), $x_1' = 0.1105$ (Fig. 6d) and with $q = 5$, $\mu = 15$, $\nu = 2,3$ (thin dashed lines) and $\nu = 4,5,6,7,8$ (thin solid lines).

For all $\mathbf{x}\in\mathcal{D}$, let the functions $e\mapsto p_{\varepsilon(\mathbf{x})}(e;\mathbf{x})$ and $e\mapsto p_{\varepsilon^{\mu,\nu,d}(\mathbf{x})}(e;\mathbf{x})$ be the probability density functions of the random variables $\varepsilon(\mathbf{x})$ and $\varepsilon^{\mu,\nu,d}(\mathbf{x})$. Figure 8 shows the graphs of functions $e\mapsto\log_{10}(p_{\varepsilon(\mathbf{x})}(e;\mathbf{x}))$ (thick solid lines) and $e\mapsto\log_{10}(p_{\varepsilon^{\mu,\nu,d}(\mathbf{x})}(e;\mathbf{x}))$ (thin solid lines) where $\mathbf{x} = (x_1,x_2,x_3)$ with $x_2 = x_3 = 0$ and $x_1 = 0.0152$ (Fig. 7a), $x_1 = 0.1018$ (Fig. 7b) and with $q = 5$, $\mu = 15$ and $\nu = 4,5,6,7$.

8. Conclusion

A method for solving the stochastic inverse problem with chaos decomposition for experimental identification of stochastic system parameters is proposed. This method is based on the use of chaos decomposition of the stochastic parameters to be identified and of the maximum likelihood principle. The convergence properties of this stochastic representation are studied through a numerical example. For the example considered, this method allows the probability density functions, the mean values, the standard deviation, the third and the fourth order moments to be identified. The approach presented in this paper can readily, and most beneficially, be extended to problems of structural dynamics.

9. References

Spanos, P, and Ghanem, R (1989) “Stochastic finite element expansion for random media”, Journal of Engineering Mechanics **115**(5), 1035–1053

Fadale, Tushar D., Nenarokomov, Aleksey V., Emery, Ashley F (1995) “Uncertainties in parameter estimation: The inverse problem”, International Journal of Heat and Mass Transfer, **38**(3), 511–518.

Shevtsov, B. M., (1999) “Backscattering and Inverse Problem in Random Media” ,Journal of Mathematical Physics, **40** (9): 4359-4373.

Capilla, J. E., Gomez, J. J., Sahuquillo, A., Franssen, H. J. W. M. H. (2000) “Stochastic Inverse Problems in Groundwater Modeling” ,Water Studies, **7**: 295-304.

Desceliers, C., and Ghanem, R., and Soize, C.(2005) “ Maximum Likelihood Estimation of Stochastic Chaos Representations from Experimental”, (accepted for publication in IJNME)

Wiener, N. (1938), “The Homogeneous Chaos” , American Journal of Mathematics, **60**: 897–936.

Ghanem, R., and Spanos, P., (1991) *Stochastic Finite Elements: A Spectral Approach*, Springer-Verlag, New York.

Soize, C., and Ghanem, R. (2003) “Physical Systems with Random Uncertainties: Chaos representations with arbitrary probability measure”,*SIAM Journal of Scientific Computing*. (in press)

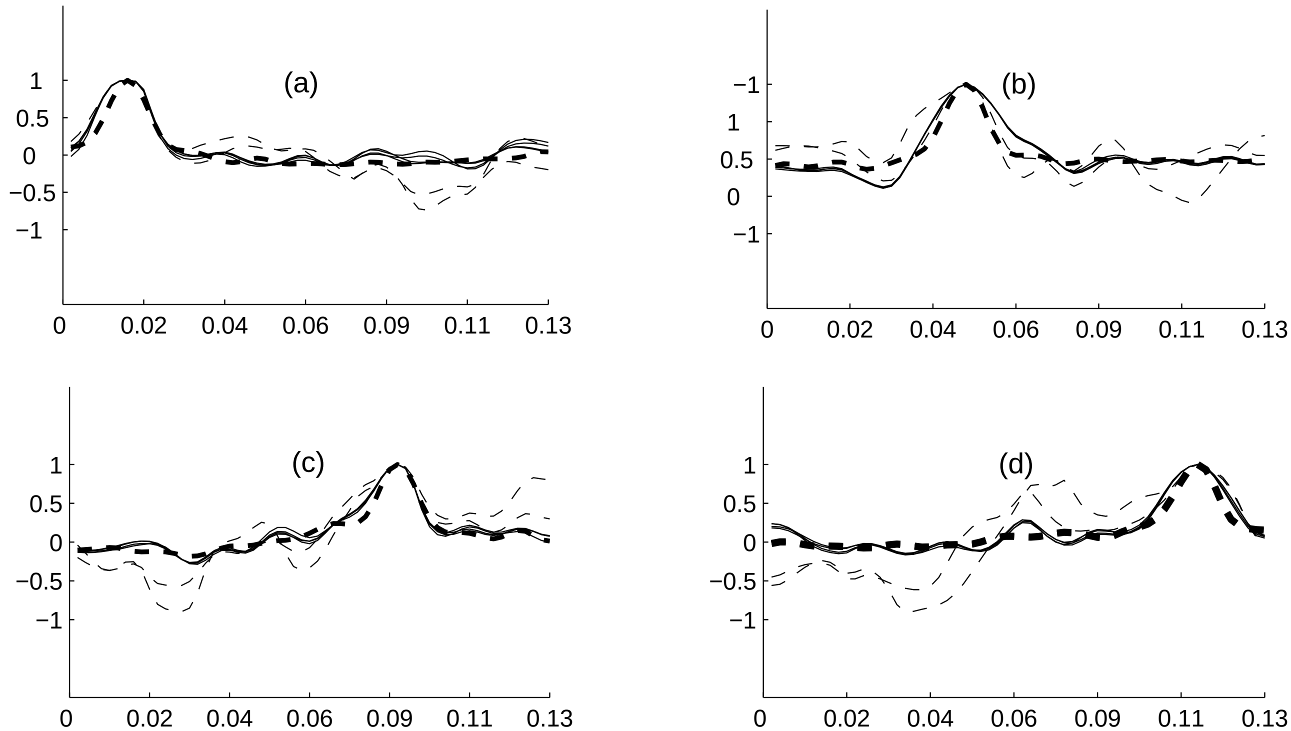

Figure 6. Graphs of functions $\mathbf{x} \mapsto E\{\varepsilon(\mathbf{x})\varepsilon(\mathbf{x}')\}$ (thick dashed lines) and $\mathbf{x} \mapsto E\{\varepsilon^{\mu,\nu,d}(\mathbf{x})\varepsilon^{\mu,\nu,d}(\mathbf{x}')\}$ where $\mathbf{x} = (x_1, x_2, x_3)$ and $\mathbf{x}' = (x'_1, x'_2, x'_3)$ with $x_2 = x_3 = 0$ and $x'_2 = x'_3 = 0$, for $x'_1 = 0.0173$ (Fig. 6a), $x'_1 = 0.0520$ (Fig. 6b), $x'_1 = 0.0888$ (Fig. 6c), $x'_1 = 0.1105$ (Fig. 6d) and with $q = 5$, $\mu = 15$, $\nu = 2, 3$ (thin dashed lines) and $\nu = 4, 5, 6, 7$ (thin solid lines). Horizontal axis: x_1. Vertical axis: $E\{\varepsilon(\mathbf{x})\varepsilon(\mathbf{x}')\}$ and $E\{\varepsilon^{\mu,\nu,d}(\mathbf{x})\varepsilon^{\mu,\nu,d}(\mathbf{x}')\}$

Marquardt D. (1963) “An Algorithm for Least-squares Estimation of Nonlinear Parameters”, *SIAM Journal Applied Mathematics*, **11**: 431–441

Serfling, R. J. (1980) *Approximation Theorems of Mathematical Statistics*, John Wiley & Sons.

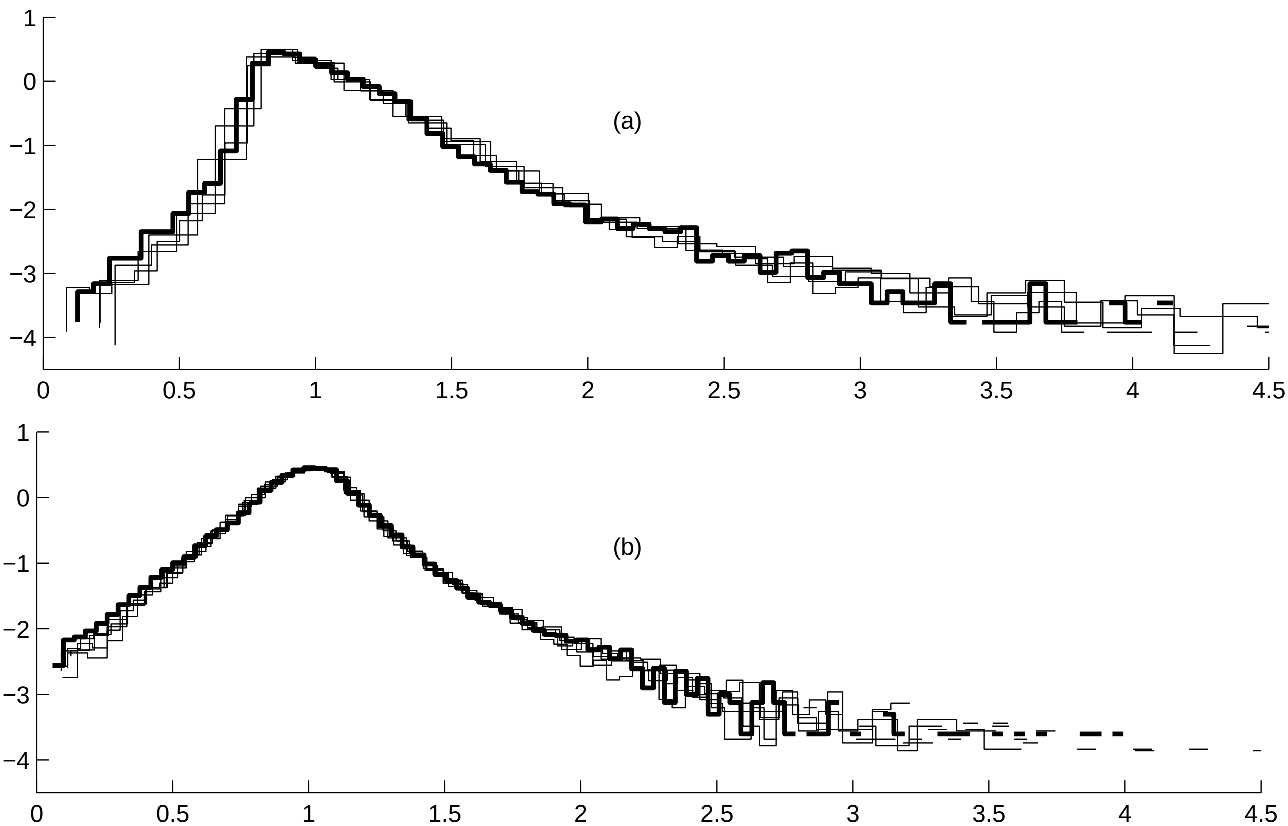

Figure 7. Graphs of functions $e \mapsto \log_{10}(p_{\varepsilon(\mathbf{x})}(e;\mathbf{x}))$ (thick solid lines) and $e \mapsto \log_{10}(p_{\varepsilon^{\mu,\nu,d}(\mathbf{x})}(e;\mathbf{x}))$ (thin solid lines) where $\mathbf{x} = (x_1, x_2, x_3)$ with $x_2 = x_3 = 0$ and $x_1 = 0.0152$ (Fig. 7a), $x_1 = 0.1018$ (Fig. 7b) and with $q = 5$, $\mu = 15$ and $\nu = 4, 5, 6, 7$. Horizontal axis: e. Vertical axis: $\log_{10}(p_{\varepsilon(\mathbf{x})}(e;\mathbf{x}))$ and $\log_{10}(p_{\varepsilon^{\mu,\nu,d}(\mathbf{x})}(e;\mathbf{x}))$.